INHOMOGENITY OF LASER-DRIVEN TECHNOLOGICAL PROCESSES
II. Material Related Inhomogenities

S. Lugomer
Ruđer Bošković Institute, Zagreb, Croatia

Keywords: laser-driven technological processes, process inhomogenity, material surfaces, metal surfaces, laser beams, L-M-I, laser-material interactions, processing technology, inhomogeneous melting, dislocation disorder, premature melting, faceted melting, rotational cells

Abstract: Inhomogenity of laser-driven technological processes, caused by the surface inhomogenity is considered. Homogeneous laser beam interacting with the (metal) surface containing irregular grains, grain boundaries, dislocations, dislocation pile-ups, inclusions of the foreign atoms etc., causes the inhomogeneous melting. Of all the possible origins of inhomogeneous surface melting, only two were considered: dislocations and the premature melting associated with the stress-intensity contours (including the rotation cells on dislocation pile-ups), and the faceted melting of polycrystalline surfaces. The first origin of premature melting is associated with laser pulses on all time scales; the last one is associated with laser pulses shorter than 10 ns.

Inhomogenost laserski-iniciranih tehnoloških procesa
II. Inhomogenost vezana na materijal

Ključne besede: procesi tehnološki laserski, nehomogenost procesov, površine materialov, površine kovin, žarki laserski, L-M-I interakcije laser-material, tehnologija obdelave, topljenje nehomogeno, nered dislokacijski, topljenje prezgodnje, topljenje facetirano, celice rotacijske

Sažetak: Razmatra se nehomogenost laserski iniciranih tehnoloških procesa, izazvanom nehomogenošću površine materijala. Homogeni laserski snop u interakciji sa (metalnom) površinom koja sadrži nepravilna zona, granice zona, dislokacije i dislokacijske nakupine, inkluzije stranih atoma i sl., izaziva nehomogeno topljenje površine. Od svih mogućih uzroka nehomogenog površinskog topljenja razmatrana su samo dva: dislokacije i prerano topljenje povezano sa konfiguracijom linije stresa (uključujući i rotacijske ćelije formirane na dislokacijskim nakupinama), i facetirano topljenje, tj. selektivno topljenje samo nekih kristalnih ploha na polikristalnoj površini. Prvi uzrok preranog topljenja javlja se kod laserskih pulseva na svim vremenskim skalama, dok se drugi javlja samo kod laserskih pulseva kraćih od 10 ns.

INTRODUCTION

The inhomogenity is introduced into laser-material interaction (L-M) either by the inhomogeneous laser beam interacting with the homogeneous (ideal) surface (i), or by the homogeneous beam interacting with the inhomogeneous (real) surface (ii). The case (i) was studied in the ref. (1), while the case (ii) is the subject of this paper.

The greatest deal of inhomogeneous L-M interactions is caused by the "real systems" i.e. the surfaces with irregular grain microstructure, lattice deformations caused by the presence of defects like, impurities, dislocations of various kind, grain boundaries, continuous or discontinuous segregates in the composite surfaces etc., as schematically shown in Fig. 1.

Areal polycrystalline surface may be assumed a surface with inhomogeneous potential barrier distribution. Such a surface shows the inhomogeneous response on the homogeneous laser beam action. The most important consequence is that the surface exhibits a premature melting in a zones around defects, thus dividing the laser spot into separate basins of various dynamics. The contours of the molten basins are therefore, defined by the premature melting barrier T_{PM}, formed around every

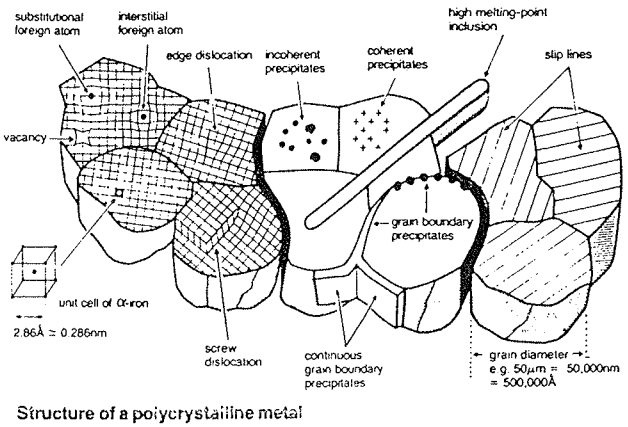

Fig. 1: Real surface of the polycrystalline metal sample. The surface is understood in a somewhat to has the thickness equal to the grain size.

particular defect. Thus, depending on the defect type and size a set of T_{PM} points will be established with characteristic that the largest defects cause the lowest T_{PM}. In other words, a homogeneous laser beam establishes the homogeneous temperature field T(x,y) on the

surface, while the surface defects establish distribution of the system transformation thresholds below T_M, which leads to local premature melting. In this way a similarity with the case (i) is established: namely, the surface shows a stochastic division into basins of solid (S) and the liquid (L) behaviour. Fig. 2. These basins are defined by the specific contours of premature melting, because the phase transition barrier is locally reduced.

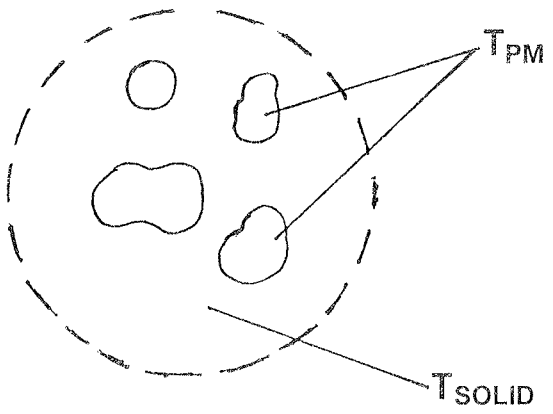

Fig. 2: Division of the laser spot into basins of the solid and the liquid response, by the contours of premature melting formed around defect places on the surface.

Since the surface defects define the point of premature melting, the surface consists of only two type of basins. The solid and the liquid one. (The basin showing vaporization has no connection to the surface defects).

Once, the basins of premature melting are established, one can introduce the pressure and temperature gradients ΔP and ΔT inside them. Introducing further their vertical and parallel components with prospect to the surface i.e. $\Delta T_{\parallel}$, $\Delta T_{\perp}$ and $\Delta T_{\perp}$, $\Delta P_{\parallel}$ and following ref. /1/, one can introduce representation of possible cases by the combination of $\Delta T_{\parallel,\perp}$ $\Delta P_{\parallel,\perp}$ gradient pairs meaning that all the physical effects discussed in ref. /1/ (for the S and L phases) are possible, in this case too.

A. GENERATION OF BASINS OF LOCAL SURFACE DYNAMICS BY SURFACE DISORDER

Dislocation Disorder:

Among all surface defects important for the inhomogeneous L-M interaction, dislocation have the most intriguing role.

Assuming a regular topological network on the ideal crystal surface, the introduction of any dislocation reflects as a local deformation of the network, i.e., as a topological disorder. An illustration of dislocation disorder is shown in Fig. 3.a,b. Fig. 3.a. represents the crystal surface with high (local) density of strongly interacting dislocations, while Fig. 3.b. shows the other kind of disorder for the similar case. Such a locally disordered surface may be corresponded with the surface of liquid, shown in Fig. 3.c. Ziman has mentioned that (in the topological sense) the liquid state can be assumed a crystal with very high number of dislocations, while the melting can be understood as a spontaneous formation of dislocations /2/.

It is well known that the elastic energy of the system connected with dislocation is proportional to the loga-

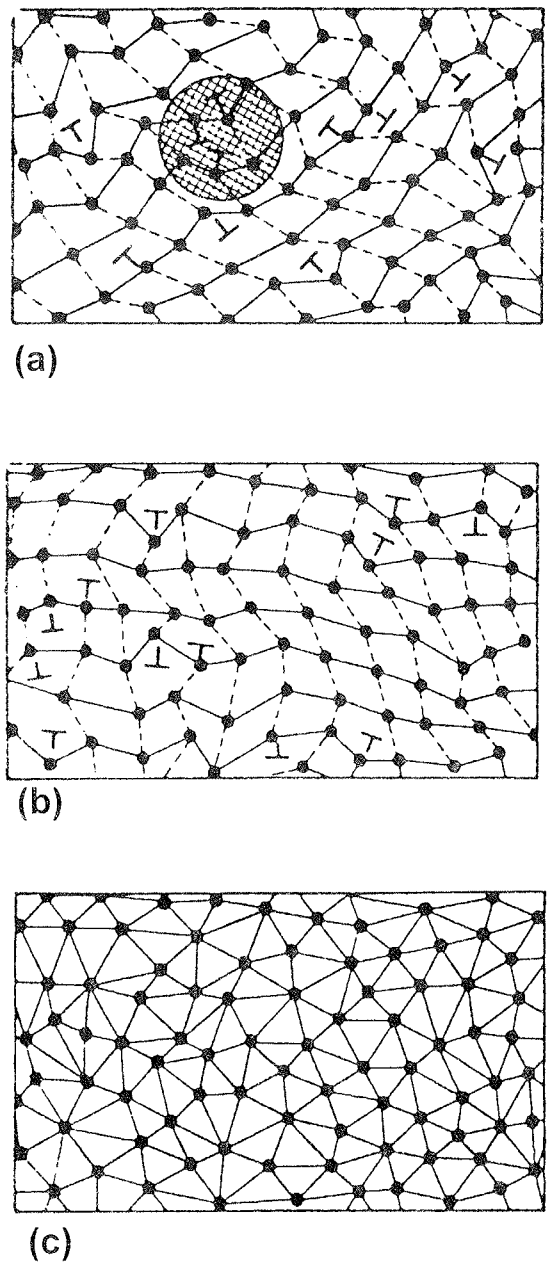

Fig. 3: Topological disorder of the crystal surface.
a) Corresponding to high density of strongly interacting dislocations.
b) Corresponding to another case of dislocation density.
c) Topological disorder of liquid.
From ref. 2.

rithm of the area taken by one dislocation. Consequently, this energy decreases as the dislocation density increases. However, this topological description has a sense only if dislocations are located at relatively large distances, so as to be easily identified /2/.

Local Density of Electronic States at the Core of Screw Dislocation

Corresponding picture to the topological one of dislocating disordered (defect) surface is the picture of local density of electronic states. Obviously, the topological lattice defect result in modified (defect) electron density of states with respect to the regular lattice, and therefore in the local forces, and in final result in different (lower) phase transition points. The best illustration is the level density of el. states calculated by Paidar for the screw dislocation in the BCC lattice. /3/

Local density of electronic states was studied taking into account a dislocation topology namely the screw dislocation with the Bargers vector (1/2) [111] in a b.c.c. lattice and using (only the s-orbits at each atomic site). For s-orbital the matrix elements of the Hamiltonian are completely determined by distances to the neighbouring atoms, and not depend on directions between them /3/. The effects of atomic disorder near a dislocation core were calculated on the hoping integrals, taking into account 30000 atoms in the topology of the screw dislocation.

The results of calculation showing local density of electronic states n(E) are given in Fig. 4. and clearly indicate

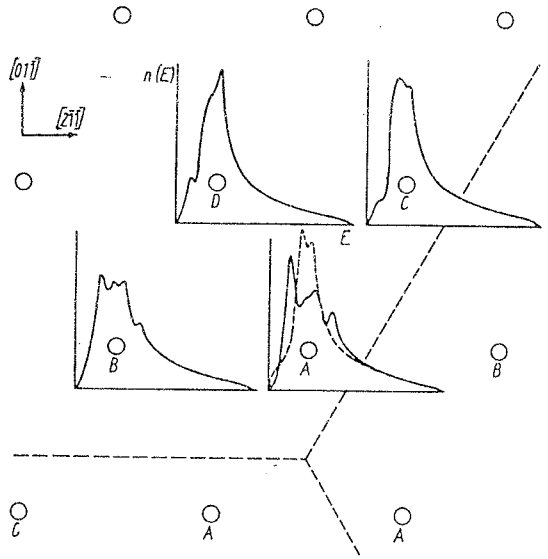

Fig. 4: Local density of electronic states for atoms in the screw dislocation core. For comparison, the local density of states for the perfect b.c.c. crystal is plotted by dashed line. The positions of atomic rows in the projection onto the (111) plane are marked by small circles. Three dashed lines radiating from dislocation centre (the projection of dislocation line), correspond to the half-planes [011] onto which the dislocation splits. From ref. 3.

the shift and the broadening of the bond as well as covering of its symmetry at the atoms close to the dislocation center. The difference in the total energy between an atom in the dislocation core and one in the perfect lattice due to shape variations of n(E) is negative /3/. Consequently, the zone around a screw dislocation is topologically defect, bounded less toughly and therefore the zone of premature melting.

Identification of the stress-intensity contours around 1,2 or more screw dislocations.

Different view of this problem is based on the stress-intensity lines associated with dislocations in the lattice. Various kinds of stress-intensity contours were found around 1,2 or more screw dislocations (in metals), which are in a strong interaction.

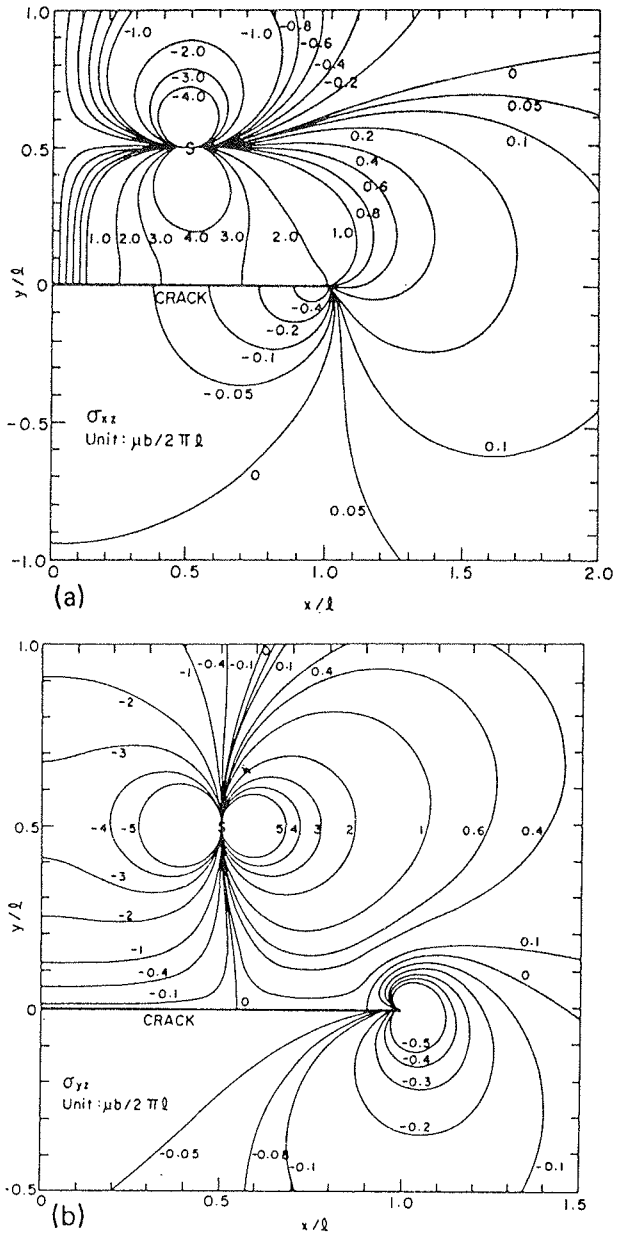

Fig. 5: Contours of stress components are induced by a **dislocation situated at (0.5l, 0.5l)**. *(a)* σ_{xz}, *(b)* σ_{yz}. *From ref. 4.*

The stress-intensity configuration modifies (decreases) a local surface forces and therefore reduces the melting point. This configuration plays a crucial role in the surface L-M interaction causing local melting and amorphization.

Very complex case of elastic interaction between general parallel screw dislocations and a surface crack was studied by Yung and Lee /4/. Assuming a complex situation of a defect surface i.e. such which contains crack(s) and the screw dislocations in the crack tip vicinity, they calculated the stress-intensity configuration in a few different topological situations calculating the stress field:

(i) induced by dislocations inside the crack

(ii) induced by lattice dislocations.

The contours of the stress components σ_{xz} and σ_{yz} (without the applied stress), for different crack size, ℓ, are given in Figs. 5.a,b. The stress-intensity contours at the crack tip are given in Fig. 6.

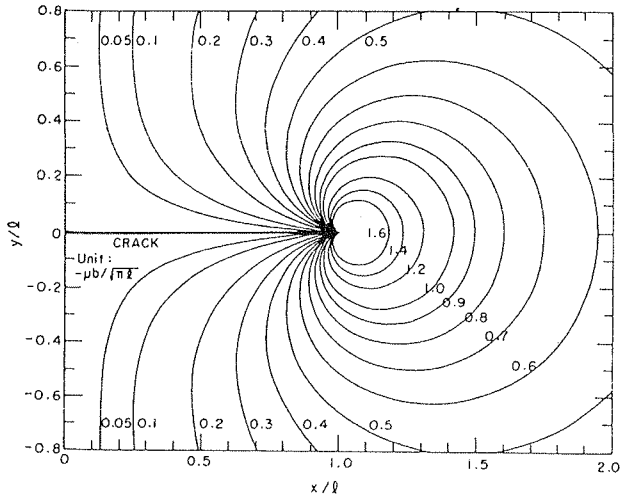

Fig. 6: Contour of the position of the dislocation to generate the same stress intensity factor (unit = $\mu b/\sqrt{\pi l}$) at the crack tip (μ = shear module, b = Burgers vector of screw dislocation). From ref. 4.

The contours of the stress-intensity factor (in the absence of applied stress), for different angles α and ϕ_0 are given in Fig. 7.a,b,c. [The angle α is the angle between the line connecting two antiparallel screw dislocations, and the base plate, while ϕ_0 is the angle between dislocations and the crack-line]. (See ref. 4.)

The contours of the stress-intensity factor determine the local surface topology which is a candidate for a premature melting in laser treatment.

Obviously, the envelope of the (premature) melting zone follows the stress-intensity lines. Since, their shape is strongly dependent on the number of interacting dislocations and their spatial location, one expects a number of shapes, usually appearing as isolated cells, some of which are rotational.

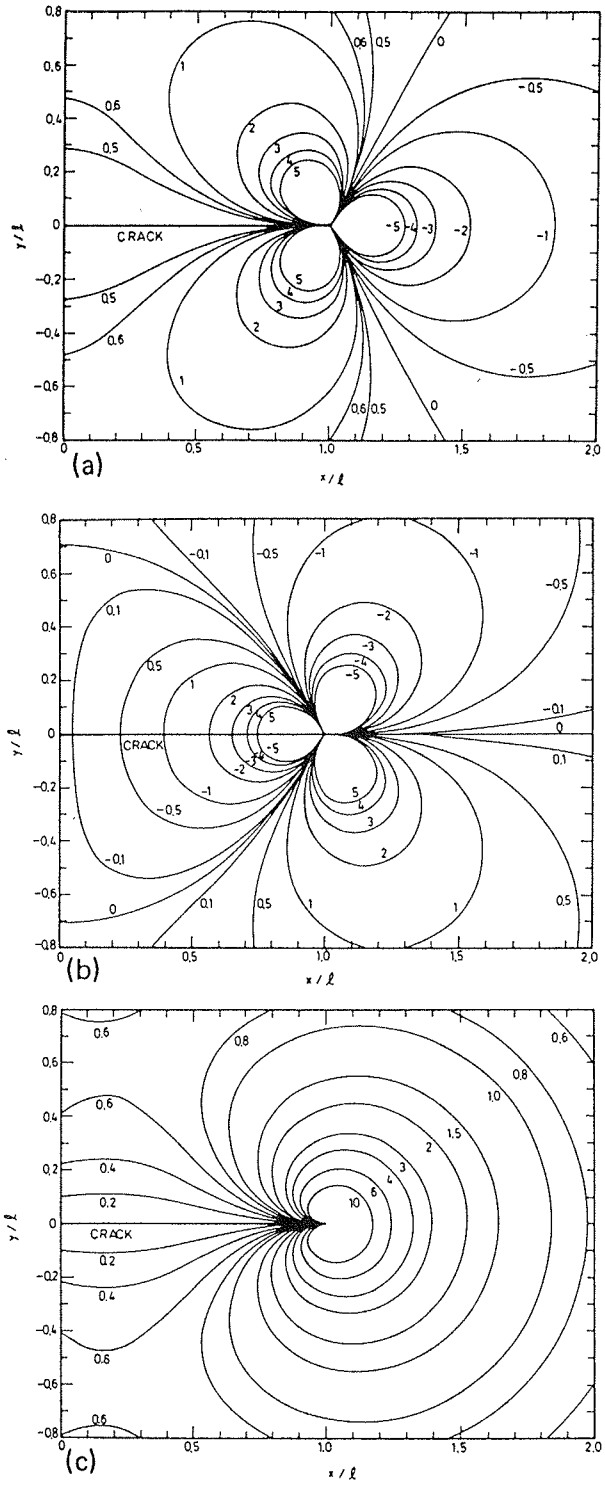

Fig. 7: Contour of the position of the dislocation dipole **to generate the same stress intensity factor** *(unit = $\mu ab/\sqrt{\pi l}$) at the crack tip. (a) α = 0. (b) $\alpha = \pi/2$. (c) $\alpha = \phi_0$. From ref. 4.*

Formation of rotational cells on dislocation pile-ups

It was recently shown that local premature melting is associated with the appearance of the surface rotational cells in shock-located crystalline metallic materials. The effect is of a general nature appearing in different kinds of shocks, and in this respect covers the specific field of laser-induced shocks.

The rotational cells are generated in crystalline metallic material (steel, Cu, A, and Ti based alloys). In shock-loaded metallic crystals the small regions are rotated relative to the neighbouring material. The disorientation of such rotated regions (rotation cells) ranges from units to dozen degrees. There are two types of RC-s: a) Crystallographic RC-s are spherical, b) At given boundaries the RC-s are imperfect, but close to spherical usually associated with crack (see the previous work of Yung and Lee).

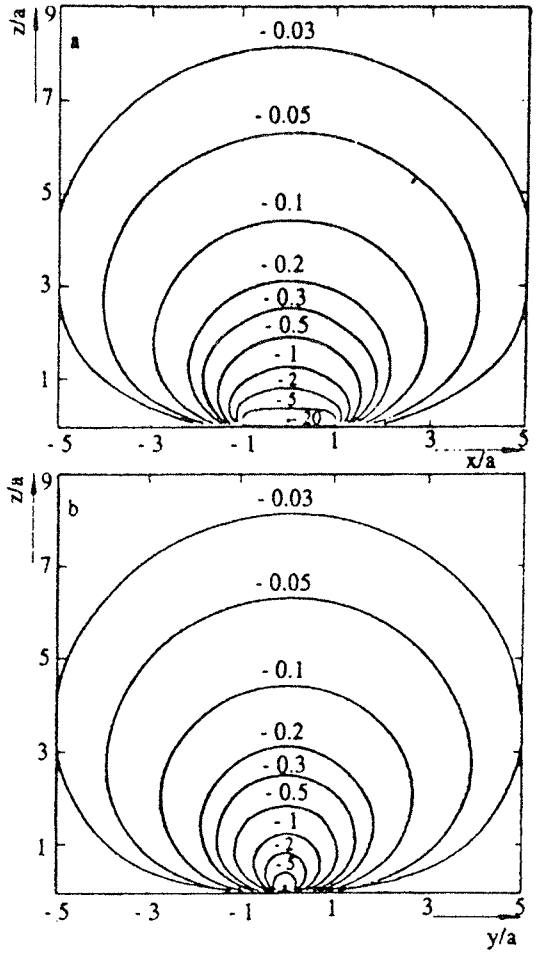

Fig. 8: *Maps of* **spatial distribution of the hydrostatic stress field** *induced by the* **π-shaped superdislocation loop** *with the edge* **segment length being** *2 a. Here we use value of G/6π (1+νB)/(1-νa) as unit for the hydrostatic stress field. (a)* **The section y=0. (b) The section x=0.** *From ref. 5. (G = shear module, ν = Poisson ratio, B = Bergers vector of large dislocation loop: B = Nb; a = dimension of a large dislocation loop.).*

The rotational cells range from one to many of them being quite disordered or ordered (organized) into chains, or some irregular formations (as we observed in laser generated shocks). An important feature of the RC-s is that they have a **resonant character** relative to the shock-load rate /5/. This effect assures within a certain (narrow) interval of shock-load-rate for each material. The physical model of the RC-s generation of Gutkin et al./5/ is based on dislocation loop pile-ups in shock loaded metallic crystals. For example, in iron and steel materials the shock wave of amplitude of ~13 GPa, a straight line of parallel rows of screw dislocations oriented along <111> directions inside grains is generated. Therefore, the ensemble of dislocation loops is introduced, and each edge screw of the dislocation loop move in the shock-wave front, while the screw-segments are immovable. The length of the screw segment increases parallel with the motion of the edge segments. This process leads to the formation of pile-ups consisting of the edge segments of the dislocation loop, when such segments are stopped by orbital (grain boundaries, particles, etc.) /5/. This process is the bases for the local appearance of the new properties, for example the local melting, which occurs near the head of a dislocation pile-up. Thus, the local amorphous phase is formed in the region near the dislocation pile-up head characterized by both high stress concentration and high latent energy density /5/.

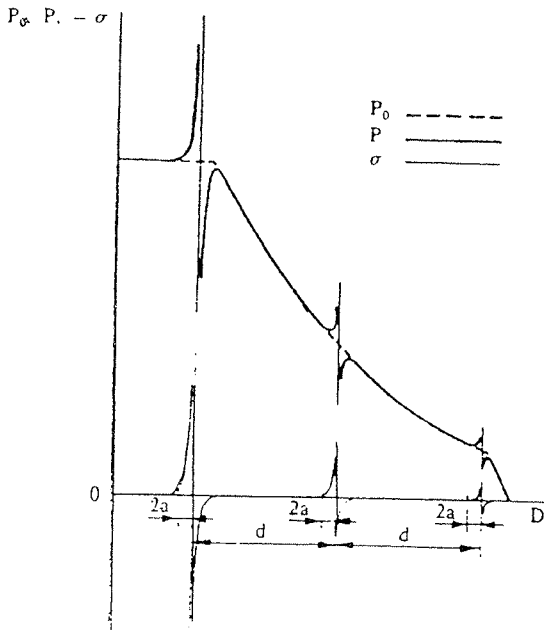

Fig. 9: **Local excitations of the shock-wave** *front* **near dislocation pile-up (schematically).** *Here the axis D intersects the head of the dislocation pile-ups and is oriented along the wave propagation direction. P denotes the mean pressure at the shock-wave front. P the effective local pressure. - σ the local pressure field induced by the dislocation loop pile-ups.* **2a the length of edge segments** *(which are perpendicular to axis D) of the dislocation loops being elements of the dislocation pile-ups.* **d the mean distance between the dislocation pile-ups.** *From ref. 5.*

The stress-field characteristics acting on the dislocation pile-up were determined for superdislocation lags consisting of N dislocations in the dislocation pipe-up. /5/

The components of the hydrostatic stress (compression) were calculated, and the result is graphically shown in Fig. 9. The effective dislocation of the elastic precursor (elastic component of the shock wave) E~10-100 ns while the time needed for the generation and 1 dislocation loop on the basis of Frank-Read mechanism is 0.5 ns, with shear stress to ~10^{-4} G (G = shear module). Thus, for the time $\tilde{t}$ (duration of elastic precursor), the pile-up consisting of 10-100 dislocation loops can be formed near the same origin The length of the pile-up is $\tilde{\ell}$ ~0.1-1 μm /5/.

Besides the compressive stress, the rotational momenta in local regions, are generated. There consequences are:

(i) a high concentration of interstational atoms within the shock-wave front, generated through anomalously high diffusion
(ii) capability of crystal-to-glass-to-crystal transformation induced by the shock
(iii) local rotations.

The resonance character of the process manifests by dependence of the process on the shock loading rate.

If the shock loading rate is small, $V<<V_{resonance}$ the intensity of the intensity of the shock more is sufficient for dislocation pile-up formation. If $V>>V_{res.}$, the shock

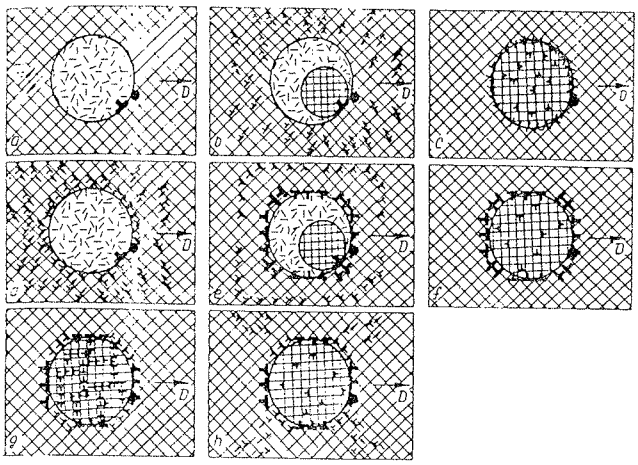

Fig. 10: Models of the formation of **crystallographic rotation cells(RCs) near dislocation pile-ups**. *(a) The* **formation of the crystallographic RC whose boundary contains the low-density ensemble of dislocations (case $V \geq V_{res.}$ abrupt front)**. *(d-g) Crystallization of the amorphous nucleus is followed by the formation of the crystallographic RC which contains the high-density dislocation ensemble (case $V \geq V_{res.}$ sloping front). (h) The same as (d-g), but dislocations "scatter" t the surrounding material (case $V \leq V_{res.}$ sloping front, short impulse). From ref. 5.*

more with a very abrupt front moves causing inhomogeneous amorphization (local, spherical amorphous zones). /5/

For $V<V_{res.}$ formation of chains was observed oriented along the shock more propagation direction. Formation of the individual rotation cells is show in Fig. 10. and formation of chains-of-rotational cells is shown in Fig. 11.

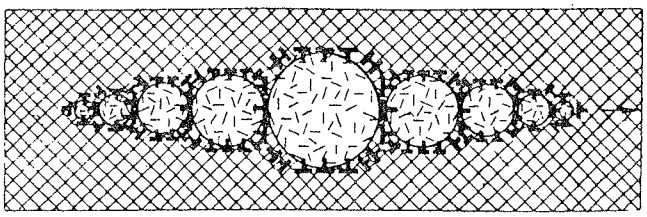

Fig. 11: Model for the formation of the chain of the **crystallographic rotation cells** *(case $V \leq V_{res.}$ sloping front,* **long impulse**). *From ref. 5.*

Dimensions of the RC-s in the chain decrease from center to the edges of the chain. Decrease of dimensions of RC-s to the left of the center occurs since interstational atom concentration decreases as the shock wave propagates through the region in which the formation of the RC-s occurs. Decrease of dimensions of RC-s to the right of the chain center occurs since only a small-density ensembles of dislocations have time to be formed at boundaries of amorphous nuclei /5/.

B. FACETED MELTING

The inhomogenity of L-M interaction a local premature melting may also appear though other reasons different from the (surface) dislocations. The polycrystalline surfaces, like those schematically shown in Fig. 1., [because of different potential on different crystallographic surfaces] may exhibit a premature melting at some surface facets and not on the others.

This effect is expected to occur in L-M interactions on the time scale below 10 ns; very fast cooling after pulse termination causes immediate freezing of the surface in which local melting stay frozen permanently. In all the other cases [i.e. for τ>10 ns time scale] a fast thermal diffusion and the heat conduction causes the melting also of the neighbour metal facets, with different crystallographic orientation, so that premature melting of only one specific facet is lost /6,7,8/.

Surface effects which are the consequence of crystal anisotropy i.e. crystal facet dependent, like for example surface faceting and melting. Surface faceting is a spontaneous decay of a crystal face into partions (facets) of other faces, (under laser pulse treatment).

The stability of surfaces is connected with the anisotropy of the surface free energy of crystals. The microscopic

mechanisms leading to surface faceting may be diverse, so long as they produce a dip in the specific surface free energy of a crystal, which generates the unstable region. Unstable vicinal surfaces facet and involve into hill-and-walley structures. Sharp edges are than present on the equilibrium crystal shape /6/. A phenomenon which is instead typical of high temperature is surface melting. It consists of preferential **thermal breakdown** of crystalline rigidity with onset of liquid-like mobility and diffusion near the surface. When present, this phenomenon leads to the formation of a stable "quasi-liquid-layer" which coats the crystal surface, and where thickness may diverge when the melting point T_m is approached from below. Surface melting has been shown to take place on a large variety of mell characterized surface faces. Generally speaking surface melting is common for weekly bounded crystals (Van der Vaals crystals), and for the poorly packed faces of any given crystal. On the contrary, the well packed surfaces of strongly bonded metals are more stable and less pure to surface melting which has been shown not to occur for Al(111), Au (111), Cu (111) etc. /6,7/

The high temperature faceting was studied by computer simulation for the vicinal surface close to Au(111). The results are shown in Fig. 12. Fig. 12.a. shows particle trajectories at low temperature for the surface configuration chosen, in this particular case a (423) vicinal with $\beta \cong 15.2°$; and reconstructed terraces. Bringing the surface in thermal equilibrium close to the bulk melting temperature, gives the result in Fig. 12.b. The steps have merged or collapsed together to form a liquid "drop" whose surface is slotted at an angle $\beta_C \sim 30°$ with respect to the (111) direction. /6,7/

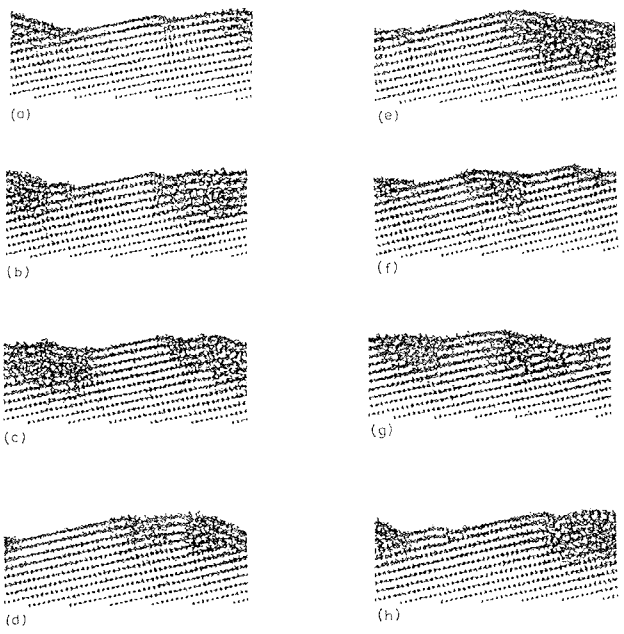

Fig. 12: Examples of fluctuations for the high-temperature faceting. The Au(534) surface is shown at T=0.99 T_m after: (a) 1.8, (b) 2.9, (c) 3.6, (d) 4.6, (e) 5.4, (f) 6.1, (g) 6.4, and (h) 7.1 ns. From ref. 6.

Among additional kinds of welting phenomena, there are prewetting (involving a jump in the thickness of the wetting layer) and incomplete wetting, where the thickness of the wetting layer saturates at some finite value. Thus, for example, the Pb(100), Ni(100) and Au(100) show only disorder at T_m, i.e. only the incomplete wetting. /6,7/

Molecular dynamics calculations for A(100) have shown a very interesting effect. While at 0,3 T_m and 0.74 T_m there is a little diffusion and the surface is in a solid phase, at 0.8 T_m and 0.99 T_m, a considerable amount of liquid diffusion exists but solid-like-islands are also present. Disorder is essentially restricted to the two topmost layers. /6,7/

CONCLUSION

Of all the possible material-related origins of inhomogenity in L-M-I, we addressed only two in this paper: dislocation disorder and the faceted melting. The first origin is associated with the laser pulses on all time scales, while the second one is associated with pulses shorter than 10 ns. Both of them couse premature melting as a local phenomena limited either to the largest stress-interesty contour (i) or to the size of the particular facet. They are the most interesting subject of intensive studies today. All the others, like local lattice distorsion because of Jan-Teller effect, chemical composition, etc. were not considered in this paper. Also, the effects caused by different light absorption in composite materials, or those containing inclusions of the foreign particles, were not the subject of this paper.

It was shown that the stress interesty contours around dislocations in the L-M interaction are the premature melting contours. Dislocation disorder of high degree usually leads to formation of dislocation pill-ups on the stress-intensity contour and to the rotational cells. Different kind of rotational cell organization on the surface (linear, irregular, etc.) was shown to appear depending on the surface stress field configuration.

In addition, the faceted crystal surface melting was discussed also. It was mentioned that (110) surfaces of fcc metals exhibit surface melting, i.e. complete wetting of the solid gas interface by the liquid at the ns and ps time scale. On the contrary, close-packed (111) surfaces of many fcc metals do not melt below T_m. The surface melting properties of (100) fcc surfaces, with on intermediate packing density between (110) and (111), are less known today.

REFERENCES

/1/ S. Lugomer; MIDEM: **1** (1994) 12.

/2/ J.M. Ziman; "Models of Disorder", Cambridge University Press, Cambridge, London, 1979.

/3/ V. Paidar; Physica Status Solidi: **B103**

/4/ R. Juang and S. Lee; J. Appl. Phys. **59** (1986) 3429.

/5/ M.Y. Gutkin, I.A. Oridko and Y.I. Mescheryakov, J. Phys. II. **3** (1993) 1563.

/6/ G. Bilalbegović, F. Ercolessi and E. Tosatti; Surface Sci. Lett. **258** (1991) L678.

/7/ G. Bilalbegović, F. Ercolessi and E. Tosatti, Surface Sci. **280** (1993) 335.

/8/ H.M. van Pixteren, B. Phuis and J.W.M. Frenken; Phys. Rev. **B49** (1994) 13798.

Dr. S. Lugomer, dipl. ing.,
Institut Ruđer Bošković
Bijenička 54, 41000 Zagreb, Croatia
tel. +385 41 45 111
fax +385 41 425 497

Prispelo (Arrived): 20.12.94 ***Sprejeto (Accepted): 31.01.95***